Transactions, **SMiRT-26**
Berlin/Potsdam, Germany, July 10-15, 2022
Division II

FRACTURE SIMULATION OF CRACKED PIPES UNDER SEISIMC LOADING

Jin-Ha Hwang[1], Yun-Jae Kim[2], Jin-Weon Kim[3]

[1] Postdoc, Korea University, Seoul, South Korea (jinhahwang@korea.ac.kr)
[2] Professor, Korea University, Seoul, South Korea (kimy0308@korea.ac.kr)
[3] Professor, Chosun University, Gwangju, South Korea (jwkim@chosun.ac.kr)

ABSTRACT

In the previous studies, the energy-based damage model was developed by simulating pipe fracture behaviour under seismic loading. The multi-axial fracture strain energy density, the parameter of energy-based damage model, was determined by experimental data under monotonic loading. Then multi-axial fracture strain energy density obtained from monotonic loading was applied to the seismic loading. The pipe fracture test under seismic loading was simulated by using energy-based damage model. The simulated results were good agreement with experimental data under high load amplitude reverse cyclic loading and displacement controlled large scale cyclic loading. However, the conservative predicted results are shown in pipe test with low load amplitude and different load ratio. In this paper, the energy-based damage model was improved by considering the effect of load amplitude and load ratio on multi-axial fracture strain energy density. The improved damage model was applied by pipe fracture test under seismic loading with two load amplitudes and two load ratios. The simulated results were compared with experimental data and validated.

INTRODUCTION

The fracture behavior for cracked pipes under seismic loading is an important part of the structural integrity for nuclear power plant. Seismic loading consists of the dynamic loading and very low cycle fatigue loading. Due to reduce fracture toughness under seismic loading, the very low cycle fatigue loading was more dominant than dynamic loading. Many laboratories were conducted full-scall pipe fracture test to observe the complex pipe behavior under very low cycle fatigue loading. The experimental approach has limitations in time, economy, and boundary condition. The effective approach is needed to observe the complicated fracture under very low cycle fatigue.

The finite element (FE) analysis method using damage model simulated pipe fracture behavior under very low cycle fatigue loading. In the previous study, the energy-based damage model was proposed to crack growth under very low cycle fatigue loading. The previous damage model was verified for cracked specimen and through-wall cracked pipe specimen. The predicted crack growth shows good agreement with experimental data for displacement-controlled large scale cyclic loading and high load amplitude fully reversed cyclic loading. However, the predicted crack growth shows conservative results compared with the experimental data under the low load amplitude fully reversed cyclic loading and different load ratio cyclic loading. This is because it is assumed that the damage model under cyclic loading is the same as the damage model under monotonic loading.

In this paper, the energy-based damage model was improved by considering the effect of load amplitude and load ratio on fracture strain energy. The fracture strain energy increased with the load amplitude and load amplitude in experimental data. The effect of load amplitude on fracture strain energy

was considered by the definition of cyclic fracture strain energy proposed by Morrow. The effect of load ratio on fracture strain energy was considered by the Manson-Coffin fatigue life curve proposed by Dowling. The proposed model predicted the pipe fracture behavior under various load amplitudes and load ratios. The predicted crack growth and failure cycle were compared with the experimental data.

PREVIOUS ENERNGY BASED DAMAGE MODEL

In the previous energy-based damage model, the fracture strain energy density, (W_f), was defined as follows:

$$\left(W_f\right) = A \cdot \exp\left(B \cdot \frac{\sigma_m}{\sigma_e} \right) = \left(W_f\right)_M \tag{1}$$

where σ_m and σ_e are the hydrostatic stress and equivalent stress; A and B are material constant determined by monotonic tensile test data. In the previous model, the fracture strain energy density was equal to monotonic fracture strain energy density, $(W_f)_M$.

The ductile damage, D, was calculated by using incremental plastic strain energy, ΔW_P, and monotonic fracture strain energy density, $(W_f)_M$. When the accumulated ductile damage was reach to critical value, D_c, the element integration point in the FE mesh was assumed to be fail. The crack growth was simulated by loss of support due to the element failure.

$$D_C = \sum \Delta D = \sum \frac{\Delta W_p}{\left(W_f\right)} = \sum \frac{\Delta W_p}{\left(W_f\right)_M} \tag{2}$$

In the previous work, it was assumed that the fracture strain energy density was the same for the monotonic loading and the seismic loading. This assumption began with the judgement that the fracture energy of seismic loading with the characteristics of very low cycle fatigue loading would be similar to the energy of the monotonic loading. The ductile fracture mechanism under monotonic loading was observed on the fracture surface of the cracked specimen under very low cycle fatigue loading. These observations support the assumption about the energy of monotonic loading and seismic loading.

However, this assumption was only suitable for the fully reversed cyclic loading with the high load amplitude (small failure cycle) and displacement-controlled large scale amplitude cyclic loading. The fully reversed cyclic loading with the high load amplitude was similar to the monotonic loading due to low fatigue characteristics. The displacement-controlled large scale cyclic loading had fracture mechanism similar to the monotonic loading due to the rapid ductile damage at failure. Therefore, it is necessary to improve the previous model for cases where the fatigue effects such as load amplitude and load ratio are dominant.

PROPOSED ENERNGY BASED DAMAGE MODEL

The improved energy-based damage model was considered by effect of load amplitude and load ratio on the fracture strain energy. The cyclic fracture strain energy was higher than the monotonic fracture strain energy experimentally and theoretically. The fracture strain energy density under very low cycle fatigue loading is given by

$$\left(W_f\right)=\left(W_f\right)_M\cdot\left(2N\right)^{\alpha}=\left[A\cdot\exp\left(B\frac{\sigma_m}{\sigma_e}\right)\right]\cdot\left(2N\right)^{\alpha} \tag{3}$$

where α are material constants; N is number of cycles. The fracture strain energy density under monotonic, $(W_f)_M$, is the same as the previous damage model. Equation (3) was satisfied with the fully reversed cyclic loading (R=-1).

The Coffin-Manson equation considering the effect of load amplitude on fatigue life is given by

$$\Delta\varepsilon_p=\left[\left(\frac{1-R}{2}\right)^{0.5}\right]\cdot\varepsilon_f\left(2N_f\right)^{c} \tag{4}$$

where $\Delta\varepsilon_p$ is plastic strain amplitude; R is load ratio; ε_f is monotonic fracture strain; c is material constant; N_f is failure cycle. The final formular for improved energy-based damage model considering the load ratio effect on fracture strain energy is given by

$$\left(W_f\right)=\left[A\cdot\exp\left(B\frac{\sigma_m}{\sigma_e}\right)\right]\cdot\left(2N\right)^{\alpha}\cdot\left[\left(\frac{1-R}{2}\right)^{\frac{-\alpha}{2c}}\right] \tag{5}$$

where β is material constant. The fracture strain energy under very low cycle fatigue loading increased with the load ratio and the failure cycle based on the fracture strain energy under monotonic loading.

EXPERIMENTAL DATA

Test material is TP316 stainless steel at room temperature, which was applied to the Korean nuclear power plant coolant water piping system. Standard tensile test data was conducted under quasi-static loading at room temperature using smooth bar specimen in Fig. 1(a). The true stress-plastic strain curve and engineering stress-strain curve are shown in Fig. 1(b). The tensile properties for test material were summarized in Table 1.

Table 1: Summary of tensile properties for TP316 stainless steel at room temperature.

Material	Yield strength	Tensile strength	Uniform elongation	Total elongation	Reduction of Area
	[MPa]	[MPa]	[%]	[%]	[%]
TP316 SS	266	616	49.9	68.3	84.6

The pipe specimen was extracted by remnant of the pipe after construction. The small pipe specimen has diameter of 72.5 mm, thickness of 8.5 mm, and length of 250 mm. The through-wall crack was inserted into the centre of the pipe in the circumferential direction. The total angle was 90 degrees including a 70 degrees EDM notch.

The pipe fracture test was performed by combining the jigs on both sides of the small pipe specimen. The loading was applied in the form of a four-point bending. The pipe test apparatus is shown in Fig. 2(b). The monotonic loading and very low cycle fatigue loading were conducted under quasi-static

conditions. The very low cycle fatigue cyclic loading consists of high load amplitude with R=-1, low load amplitude with R=-1, and different load ratio (R=-0.5). The pipe fracture test data under monotonic and cyclic loading were summarized in Table 2. The load and crack mouth opening displacement (CMOD) were measured by the load cell and the extensometer. The crack growth was calculated as an averaged value depending on the thickness using Zahoor method.

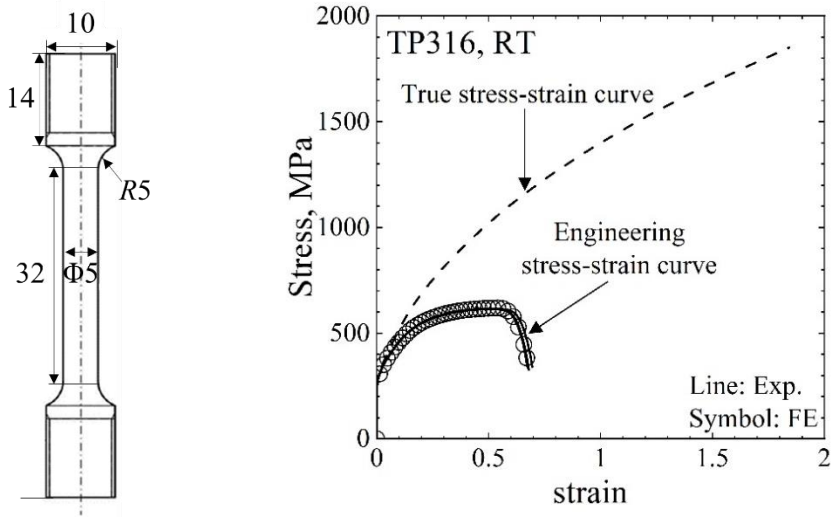

(a) (b)

Figure 1. (a) Standard smooth bar tensile specimen and (b) true stress-plastic strain and engineering stress-strain curve.

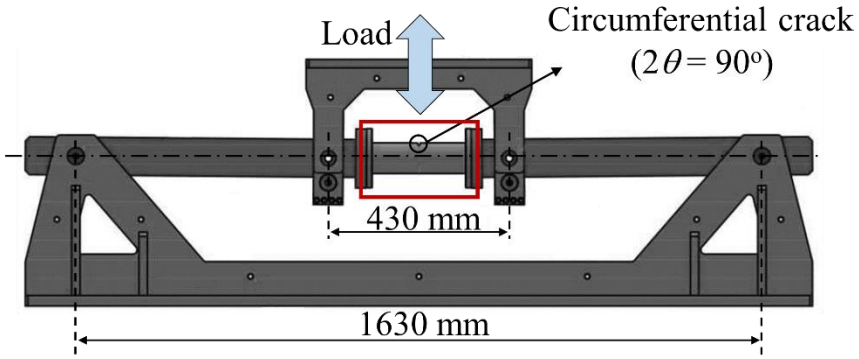

Figure 2. Four-point bending pipe test apparatus

Table 2: Summary of through-wall cracked pipe test data under monotonic loading and very low cycle fatigue loading.

Material	Test ID	Loading condition	R	P_{max}/P_M	Maximum load, P_{max}	N_f
TP316 SS	SS-M	Monotonic loading	1	1	68.3	1
	SS-Base		-1	0.85	24.8	12
	SS-A		-1	0.75	21.9	36

	SS-R	Very low cycle fatigue loading	-0.5	0.85	24.8	53

DETERMINATION OF DAMAGE MODEL

Monotonic fracture strain energy

The monotonic fracture strain energy was determined by simulating the engineering stress-strain curve using FE mesh in Fig. 3(a). As shown in Fig. 1(b), the predicted engineering stress-strain curve (symbol) was good agreement with the experimental data (line). The stress triaxiality and plastic strain energy was extracted at centre of the FE tensile mesh. The averaged stress triaxiality and plastic strain energy up to failure are shown as one point in the Fig. 3(b). The material constant, *A* and *B*, in Eq.(a) was determined by using one point from FE tensile analysis and strain hardening component. The monotonic fracture strain energy is given by

$$\left(W_f\right)_M = 8521 \cdot \exp\left(-2.18 \cdot \frac{\sigma_m}{\sigma_e}\right) \tag{6}$$

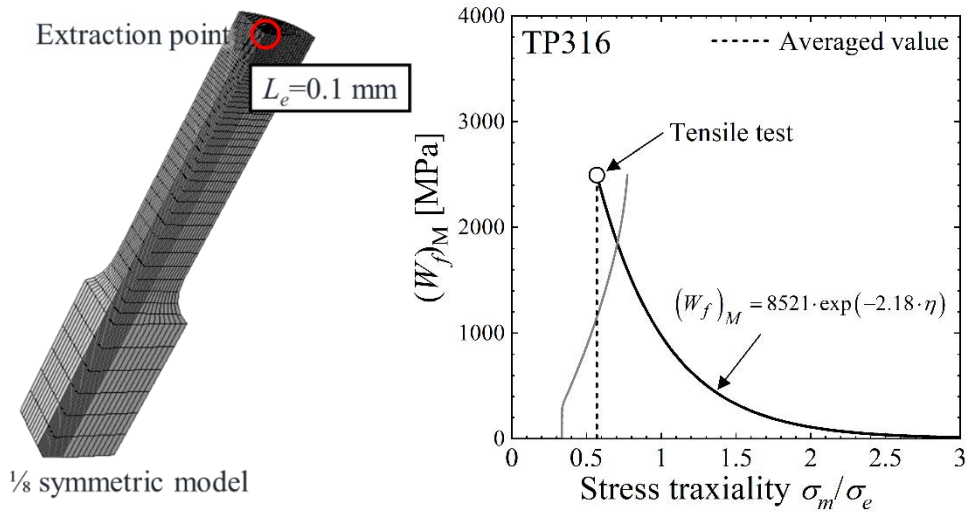

(a) (b)

Figure 3. (a) FE tensile mesh and (b) monotonic fracture strain energy.

The critical damage value, D_c, is determined by simulating the pipe fracture behavior under monotonic loading. Figure 4 shows the FE pipe mesh using crack growth simulation. The FE pipe mesh was applied by the C3D8 (3-D 1st order) element. The crack growth region consisted of about 0.6 mm cubic element. Figure 5 compare the FE simulation results with the experimental pipe test data under monotonic loading. When the D_c was 0.2, the maximum load and crack extension for cracked pipe under monotonic condition were simulated similarly to the experimental data. The Dc determined by monotonic pipe test data was equally applied to the pipe crack growth simulation under very low cycle fatigue loading.

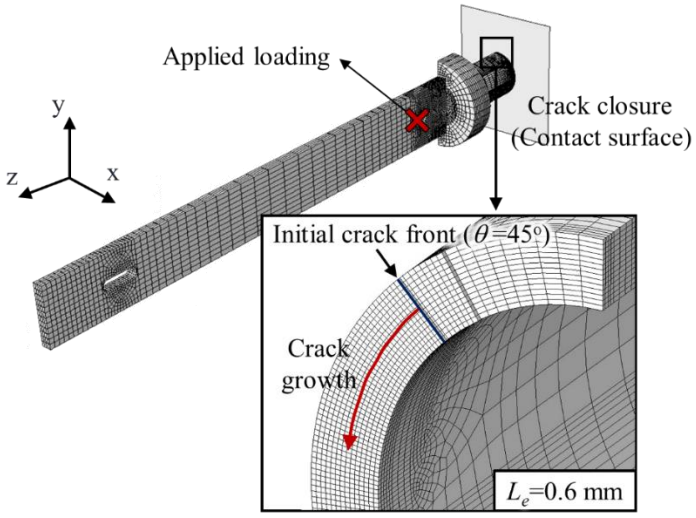

Figure 4. FE pipe mesh considering the quarter symmetric condition.

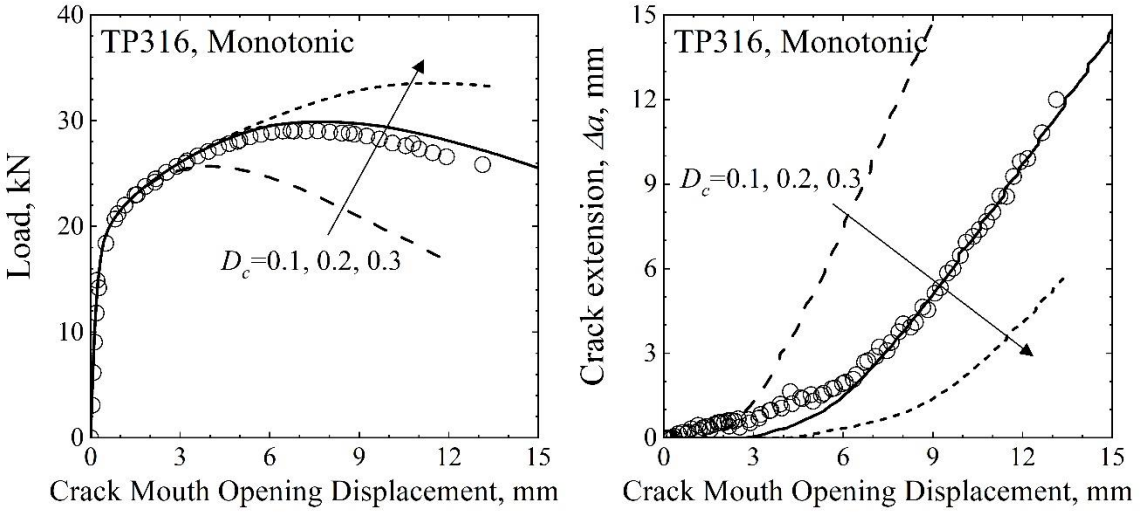

Figure 5. Comparison of FE pipe simulation with the experimental pipe test data under monotonic loading: (a) load-CMOD curve and (b) crack extension-CMOD curve.

Fracture strain energy considering the effect of load amplitude and load ratio

The effect of load amplitude on fracture strain energy was considered by the material constant, α, in Eq.(3). The α was obtained in the relationship between the plastic strain energy per cycle, ΔW_p, and the failure cycle, N_f. The failure cycle was calculated as the ANL fatigue life curve contained in the NUREG CR-6909. The plastic strain energy per cycle was calculated as the change in the averaged plastic strain energy up to failure cycle using the FE analysis. Figure 6 shows the relationship between the plastic strain energy per cycle and the failure cycle. The ΔW_p linearly decreases on the log scale with the failure cycle. The relationship between the material constant, α, and the plastic strain energy per cycle, ΔW_p, is given by

$$\Delta W_p = \frac{W_f}{N_f} = \frac{K\left(N_f\right)^{\alpha}}{N_f} = K\left(N_f\right)^{\alpha-1} \tag{7}$$

Therefore, the material constant, α, is determined to be 0.04 based on the Fig. 6.

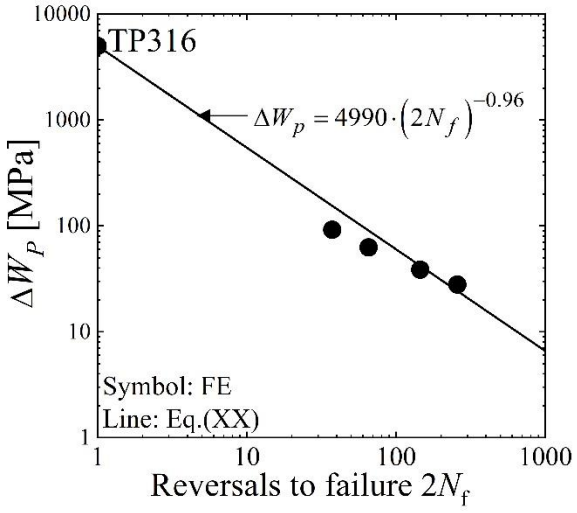

Figure 6. Figures should be centred and followed by a numbered caption.

The effect of load ratio, *R*, on fracture strain energy was considered by the material constant, *c*, in Eq.(4). The material constant, c, is the exponent of the low cycle fatigue life curve in Eq.(4). The *c* was obtained as -0.523 from the ANL fatigue life curve in NUREG CR-6909. Finally, the improved energy-based damage model is expressed as follows:

$$\left(W_f\right) = \left[8521 \cdot \exp\left(-2.18 \cdot \frac{\sigma_m}{\sigma_e}\right)\right] \cdot \left(2N\right)^{0.04} \cdot \left[\left(\frac{1-R}{2}\right)^{0.04}\right], \; D_c = 0.2 \tag{8}$$

SIMULATION RESULTS

Figure 7(a) compares predicted results under fully reversed cyclic loading with experimental data. For the high load amplitude case, predicted results using both the previous and the proposed model are well agreement with experimental crack growth data. However, for the low load amplitude case, the predicted result using the proposed model is slower than the previous model. Figure 7(b) compares predicted results under different load ratio case (*R*=-0.5) with experimental data. There is no significant different in simulated crack growth between previous model and proposed model without considering load ratio (*R*=-1), but the proposed model considering load ratio (*R*=-0.5) shows absolutely improved simulated results. Table 3 summarizes the comparison of experimental failure cycle with the predicted failure cycle depending on the damage model.

CONCLUSION

The previous energy-base damage model was improved by considering the effect of load amplitude and load ratio on fracture strain energy. The previous and improved energy-based damage model was applied by simulating the circumferential through-wall cracked pipe for TP316 under load controlled cyclic loading with different load amplitudes and load ratios. The improved model shows better predicted results than the previous model in all pipe experiment.

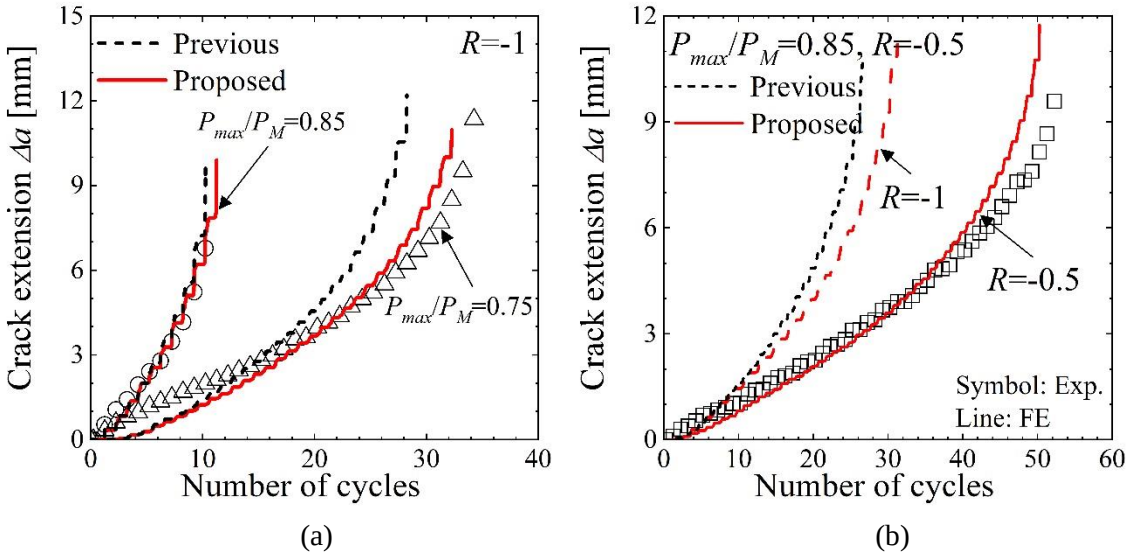

Figure 7. FE pipe crack growth simulation results depending on the damage model: (a) R=-1 and (b) R=-0.5.

Table 3: Summary of failure cycle: experiment data and FE simulation results.

Material	Test ID	R	P_{max}/P_M	Experimental failure cycle	Previous $(N_f)_{FE}$	Proposed $(N_f)_{FE}$
TP316	SS-Base	-1	0.85	12	11	12
	SS-A	-1	0.75	36	28	32
	SS-R	-0.5	0.85	53	28	51

REFERENCES

Morrow, J. (1965). Cyclic plastic strain energy and fatigue of metals. In *Internal friction, damping, and cyclic plasticity*. ASTM International.

Hwang, J. H., Youn, G. G., Kim, Y. J., & Kim, J. W. (2020). Fracture Modeling Of Cracked Pipe Under Monotonic And Cyclic Loading. *International Journal of Mechanical Sciences*, *183*, 105837.

Hwang, J. H., Kim, H. T., Kim, Y. J., Nam, H. S., & Kim, J. W. (2020). Crack tip fields at crack initiation and growth under monotonic and large amplitude cyclic loading: Experimental and FE analyses. *International Journal of Fatigue*, *141*, 105889.

Hwang, J. H., Kim, Y. J., & Kim, J. W. (2022). Energy-Based Damage Model Incorporating Failure Cycle and Load Ratio Effects For Very Low Cycle Fatigue Crack Growth Simulation. *International Journal of Mechanical Sciences*, 107223.

Kim, J. W., Do Kweon, H., & Kim, Y. J. (2021). Failure behavior of SA508 Gr. 1a LAS and SA312 TP316 SS pipes with a circumferential through-wall crack under large amplitude cyclic loads. *Thin-Walled Structures*, *161*, 107524.